Sintering and characterization of a hydroxyapatite matrix and hydroxyapatite matrix nanocomposites

Nelson H. A. Camargo*, Eliakim E. G. de Borba, Priscila F. Franczak, Enori Gemelli

Universidade do Estado de Santa Catarina – UDESC, Technological Sciences Center – CCT, Mechanical Engineering Department – DEM, Materials Science and Engineering Program – PGCEM, Joinville, Brazil

*Corresponding author, Tel: (+55) 4740097701; E-mail: nelson.camargo@udesc.br

Received: 23 June 2015, Revised: 29 November 2015 and Accepted: 22 September 2016

DOI: 10.5185/amlett.2017.6032
www.vbripress.com/aml

Abstract

Microporous calcium phosphate biomaterials are known for their physical and biological applications. Among the best known are the stoichiometric hydroxyapatite (HA) and tricalcium phosphate (TCP). This is because these biomaterials exhibit chemical and crystallographic compositions which are similar to that found in bones and teeth. The use of nanotechnology enables obtaining calcium phosphate nanostructured powders and calcium phosphate nanocomposite matrix formed by a second nano phase of type SiO_2, TiO_2, Al_2O_3-α, ZrO_2, Mg. Different methods and techniques for the synthesis and preparation of nanostructured powders and biomaterials are noted in the literature, but it is known that not all lead to the same results. Calcium phosphates nanostructured biomaterials are a new class of biomaterials which provide new physical, morphological, nanostructural and microstructural features with interconnected microporosity which are promising to wettability, capillary action, cell adhesion and proliferation on the surface of grains and micropores. Based on research of these biomaterials, it has been found that they show potential applications in traumatology, orthopedic and dental applications in reconstruction, defects and bone tissue repairing, implants attachment and dental remineralization treatment. This study was aimed at the sintering and characterization of an HA matrix and three nanocomposite biomaterials with 5% by volume of the respective second phases: SiO_2, ZrO_2 and Al_2O_3-α in the HA matrix. The HA powder and nanocomposite HA/SiO_2 were sintered at 1100°C/2h. HA/ZrO_2 nanocomposite powder followed two sintering conditions: a temperature of 1100°C/2h and the other, at 1300ºC/2h. HA/Al_2O_3-α nanocomposite powder was only sintered at 1300ºC/2h. The biomaterials were characterized by scanning electron microscopy, X-ray diffraction and open porosity and hydrostatic density were also determined by applying the Arthur method. The results are encouraging and show for HA, HA/SiO_2, HA/ZrO_2 biomaterials (obtained by sintering at 1100°C) interconnected microporous microstructures, formed by fine grains which are favorable for the expected wettability and capillarity characteristics. Copyright © 2016 VBRI Press.

Keywords: Hydroxyapatite, nanocomposite, sintering, microstructure.

Introduction

The use of nanotechnology makes it possible to obtain nanostructured powders of calcium phosphate and calcium phosphate matrix nanocomposite. Nanocomposites are formed by a nanometric second phase, consisting of SiO_2 TiO_2, Al_2O_3-α, ZrO_2, dispersed in the hydroxyapatite matrix, which are typically prepared by different methods and nanostructured powder production techniques, but it is known that not all lead to same results [**1-5]**.

Calcium phosphate nanostructured biomaterials are a new class of biomaterials that offer new physical, morphological, microstructural and nanostructural characteristics, formed by interconnected microporosity. These characteristics are promising for wettability, capillary action, cell adhesion and proliferation on the surface of grains and micropores. The application of these biomaterials have been researched and have shown immense potential applications in traumatology, orthopedic and dental applications, repairing defects and bone reconstruction, implants attachment and dental remineralization treatment **[6-11]**.

This study was aimed to evaluate the sinterability of hydroxyapatite matrix nanostructured powders (HA) and four compositions of nanocomposite powders with 5% by volume of the respective second phase: SiO_2; Al_2O_3-α and ZrO_2 in the HA matrix. Two sintering conditions were used: first condition was used to HA matrix powder and HA/SiO_2 and HA/ZrO_2 nanocomposites, which were sintered at a temperature of 1100°C/2h, and the second condition for nanocomposite powders with HA/Al_2O_3-α and HA/ZrO_2, which were sintered at a temperature of 1300ºC/2h. The objective was to evaluate the influence of the second phase and sinterability temperature on the physical, microstructural and nanostructural characteristics of biomaterials obtained from the two sintering conditions.

The scanning electron microscopy helped to evaluate the biomaterial microstructural, X-ray Diffractometry (XRD) technique served for crystallographic evaluation and the Arthur method was used to determine the open porosity and hydrostatic density.

Experimental

Nanocomposites and HA powders were provided by the Biomaterials' Group from Universidade do Estado de Santa Catarina - UDESC (Brazil). HA powder was obtained by wet synthesis method **[12]**. Nanocomposite powders were prepared in high energy attritor mill, as described by **[12]**. The powders recovered after the attritor mill were dried and sieved in mesh 100µm and subsequently compressed into a metal matrix with dimensions of 12mm in height and 5 mm in diameter. The compaction of the powders was performed with a load of 30MPa, at a compression rate of 1 mm/min in the compacting machine. The samples obtained from compression underwent sintering inside of muffle furnace camera, brand Lindeberg. Powder sintering was carried out according to two conditions: first at temperature of 1100°C/2h for HA specimens, HA/SiO_2, HA/ZrO_2 and second condition at temperature of 1300ºC/2h for HA/Al_2O_3-α and for HA/ZrO_2 specimens. The specimens recovered from the two sintering conditions were prepared for characterization studies by scanning electron microscopy (SEM), X-ray diffraction and finally hydrostatic density (d_h) and open porosity (PA) using the Arthur method [**13**] was examined. The theoretical density(d_{th}) of the nanocomposite biomaterials was also determined. Microstructural characterization was performed with the help of electronic scanning microscopy, with Field Effect (Field Emission Gun - FEG), JEOL, JSM-6701F model, by secondary electron system (SE) with 6mm working distance and 15 kV electrons acceleration voltage. Small fragments obtained from the fracture of biomaterials were analyzed. The X-ray diffractometry (XRD) served on crystallographic characterization of biomaterials. In this study a SHIMADZU X-ray diffractometer model XRD LAB X- 6000, with anti-cathode copper tube, was used. To obtain the X-rays diffraction, a 40kV voltage with a current of 30mA was used, maintaining the scanning angular range from 20° to 55°, at a goniometer speed of 2º/min with a function of 2θ. For the determination of open porosity (%) and hydrostatic density (g/cm^3), the Arthur Method was used **[13]**. This method was performed by measuring the weight of air-dried samples (Par), then weight of soaked specimen in xylene to air (Pxa); later weight of the specimen soaked in xylene immersed in distilled water (Pxe). After this, hydrostatic density calculations are carried out by means of equation 1 and percentage open porosity in equation 2.

Hydrostatic density $$dh = \frac{Par.de}{Pxa - Pxe} \quad (1)$$

Open porosity % $$P.A. = \frac{(Pxa - Par).de}{(Pxa - Pxe).dx}.100 \quad (2)$$

Results and discussion

The fracture surfaces result of HA, HA/SiO_2 and HA/ZrO_2 biomaterials sintered at temperature 1100°C/2h revealed in their micrographs that the microstructures microporous are interconnected, formed by fine grains. If the micrographs are compared, a microstructure similarity between the biomaterials can be observed, as shown in **Fig. 1, 2** and **3**. Another finding was the fracture mode, predominantly intergranular form for HA biomaterial and HA/SiO_2 and HA/ZrO_2 nanocomposites. This result can be explained by the microporosity present in the biomaterial microstructure. In the case of nanocomposites that can be explained by the presence of microporosity and second phase in intragranular position, inside hydroxyapatite matrix, which contributed to the reduction of grain size and embrittlement of grain boundaries interfaces, favoring intergranular fracture mode, as shown in **Fig. 1, 2** and **3**. This fracture mechanism has also been observed by other authors who synthesized HA matrix nanocomposite biomaterials **[2, 7, 10, 14]**.

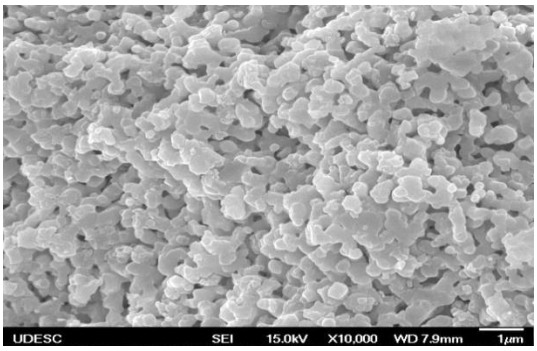

Fig. 1. Microporous microstructure of pure HA at 1100°C/2h.

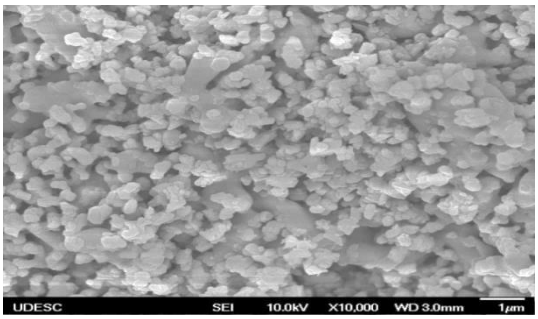

Fig. 2. Microporous microstructure of HA/SiO_2 5% by volume at 1100°C/2h.

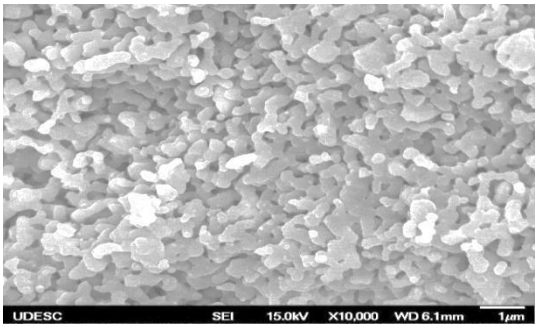

Fig. 3. Microporous microstructure HA/ZrO_2 5% by volume at 1100ºC/2h.

The result of HA/Al_2O_3-α biomaterial, sintered at 1300ºC/2h, revealed in their micrograph an interconnected microporous microstructure, clearly demonstrating that the sintering temperature of the biomaterial at 1300ºC/2h resulted in grains coalescence, and favors the HA matrix sinterability (**Fig. 4**).

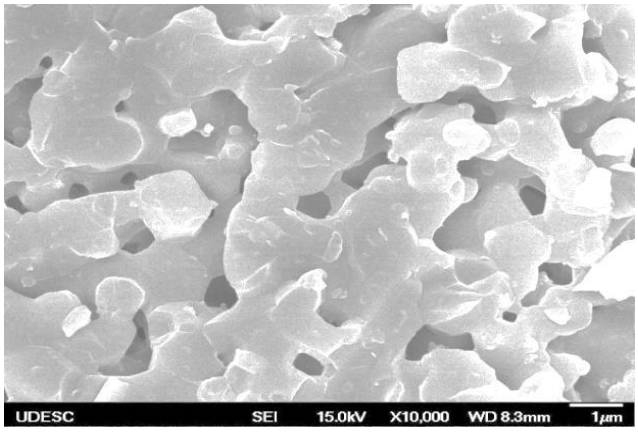

Fig. 4. Microporous microstructure HA/Al_2O_3 5% by volume at 1300ºC/2h.

If this result is compared with that obtained for the HA matrix, sintered at 1100ºC/2h (**Fig. 1**), it is clearly observed grains coalescence and there is better biomaterial sinterability.

This result is associated with increased of biomaterial sintering temperature and by the presence of α-alumina nanometric second phase in the hydroxyapatite matrix inter-intragranular position, which has an influence on the kinetics of interfacial diffusion between HA matrix and second phase during the sintering process of the biomaterial **[1, 14]**.

Micrographs revealed for the HA/ZrO_2 nanocomposite biomaterial, sintered at 1300ºC/2h, a dense microstructure, as shown in **Fig. 5**, indicating that the presence of ZrO_2 second phase in HA matrix promoted the biomaterial sinterability, closing microporosity and grain boundary interface connection.

Another observation was the presence of fine grains in lighter color in the HA matrix grain boundaries, indicating the presence of ZrO_2 and TCP-β grain, occurred as interfacial diffusion and formation of TCP-β phase during biomaterial sintering, as shown in **Fig. 5**.

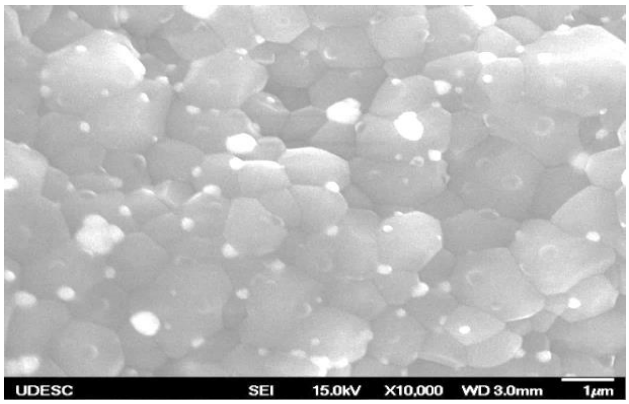

Fig. 5. Dense microstructure HA/ZrO_2 5% by volume at 1300ºC/2h.

X-ray diffraction (XRD) technique was used to identify the phases present at the different compositions of biomaterials sintered. **Fig. 6** shows the result of X-ray diffraction obtained on the pure HA biomaterial (matrix). Note the presence of representative diffraction peaks of stoichiometric hydroxyapatite phase with hexagonal crystal system and main diffraction plane (211). This result shows that a temperature of 1100°C/2h did not change the crystal structure of HA matrix.

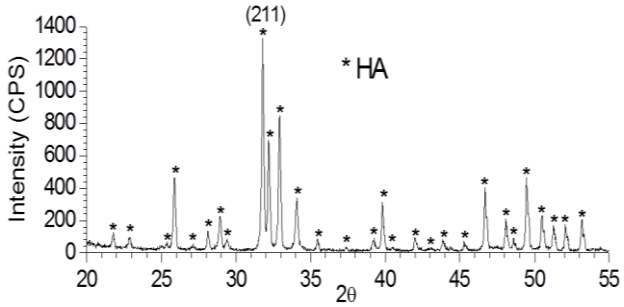

Fig. 6. X-ray diffraction pattern obtained on pure HA biomaterial at 1100°C/2h.

Fig. 7 illustrates the X-ray diffraction pattern obtained on the HA/SiO_2 5% nanocomposite biomaterial. The XRD pattern shows representative peaks of HA and TCP-β phase with rhombohedral crystal system and main diffraction plane (021). The presence of TCP-β phase is associated with the SiO_2 nanometric second phase in inter-intragranular position in the HA matrix. Another observation was the intensity reduction of hydroxyapatite phase diffraction peaks, when this result (**Fig. 7**) is compared with the X-ray diffraction pattern obtained on HA (**Fig. 6**). This result is associated with the presence of the silica second phase in inter-intragranular position in the hydroxyapatite matrix, which during nanocomposite biomaterial sintering destabilized HA phase, occurred due to the interfacial diffusion of Ca ions in grain boundaries, promoting formation of TCP-β phase, case already observed by other authors **[2, 9, 14]**.

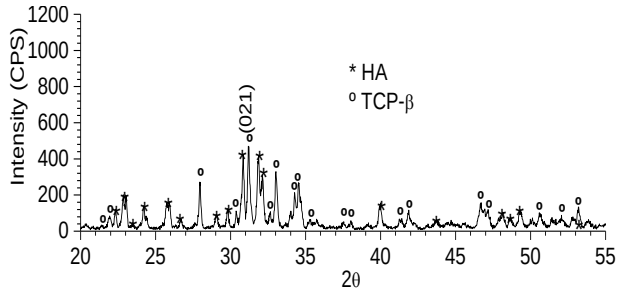

Fig. 7. X-ray diffraction pattern obtained on the HA/SiO_2 biomaterial 5% by volume at 1100°C/2h.

The presence of a second phase of nanometric order in inter-intragranular position in HA matrix acts as a catalyst and modifier of the decomposition rate of HA phase, causing the phase transformation of the TCP-β, CaO and other phases, depending on the biomaterial composition and sintering temperature [**1, 2, 9, 14-17]**.

Fig. 8 shows the diffraction pattern obtained on the HA/ZrO_2 nanocomposite biomaterial, sintered at 1100°C/2h. The representative peaks of zirconia and hydroxyapatite phase can be seen here.

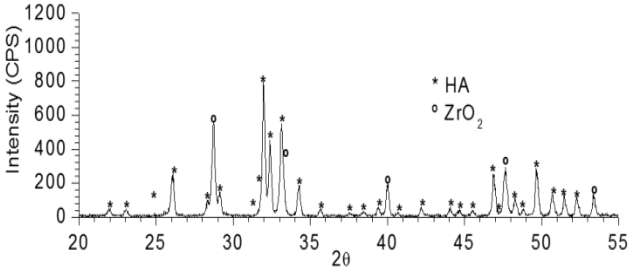

Fig. 8. X-ray diffraction pattern obtained on the HA/ZrO_2 biomaterials 5% by volume at 1100°C/2h.

There has been also a slight reduction in the intensity of the diffraction peaks for the HA phase, when this result (**Fig. 8**) is compared with those obtained for HA matrix (**Fig. 6**). Therefore, there is no presence of diffraction peaks of TCP-β or CaO phase, indicating that the presence of 5% by volume of zirconia phase and sintering at 1100°C/2h not destabilized phase hydroxyapatite.

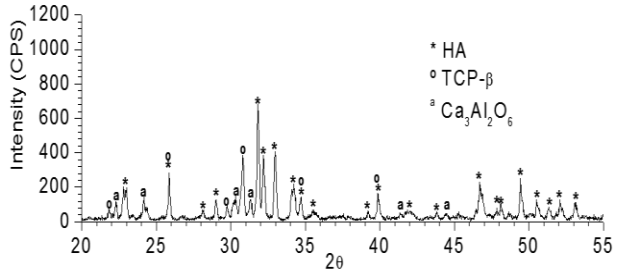

Fig. 9. X-ray diffraction pattern obtained on the HA/Al_2O_3-α biomaterials 5% by volume at 1300°C/2h.

The result of HA/Al_2O_3-alpha biomaterial revealed in their X-ray diffraction the presence of representative peaks of HA, TCP-β and calcium aluminate ($Ca_3Al_2O_6$) phase, as shown in **Fig. 9**, case previously observed by others authors **[7, 14]**.

There was also a reduction in the intensity of the HA phase diffraction peaks, when this result (**Fig. 9**) is compared with the results obtained for HA matrix (**Fig. 6**). As previously explained, this reduction in the peaks intensity is associated with the presence of the second phase nanoscale in inter-intragranular position in the HA matrix, which leads to destabilization of HA phase at high temperatures, releasing Ca ions by interfacial diffusion process to new phase formation, modifying the grain boundaries interfaces and crystallinity, leading to reduction of peak intensity of HA phase, case already observed by other authors **[1, 14]**.

Fig. 10 shows the X-ray diffraction pattern obtained on the HA/ZrO_2 nanocomposite biomaterial, sintered at 1300ºC/2h. It can be seen phase diffraction peaks of HA, ZrO_2 and low intensity peaks of TCP-β phase. As explained above, the increase in temperature and the presence of the nanoscale second phase inside the HA matrix leads to destabilization of the HA to forming TCP-β, CaO among other phases, depending on the nature of the second phase present in the HA matrix and sintering temperature applied. It is known from previous studies for the case of HA/ZrO_2 composite biomaterials, sintered at high temperatures, the formation of TCP-β, CaO and $CaZrO_3$. The formation of these phases occur by interfacial diffusion process in grain boundaries through destabilization of HA phase, release of Ca ions, formation of CaO and CaO destabilizes zirconia by reacting $CaO + ZrO_2 = CaZrO_3$ as described by **[17, 18]**.

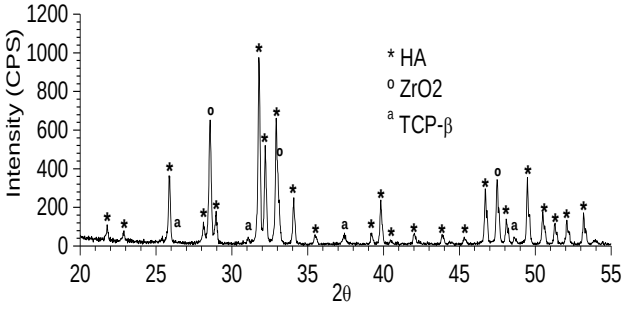

Fig. 10. X-ray diffraction pattern obtained on the HA/ZrO_2 biomaterials 5% by volume at 1300ºC/2h

The result of this study showed only the presence of HA phase, ZrO_2 and low intensity peaks of TCP-β phase, but did not show the presence of $CaZrO_3$ compound, which may be related to the low concentration of the ZrO_2 second phase inside HA matrix. Results of theoretical density (d_{th}), hydrostatic density (d_h) and open porosity (PA) are shown in **Table 1**. The results of theoretical density presented similar observations between the nanocomposite biomaterials. This can be explained by the small concentration of nanometric second phase within the compositions. With respect to hydrostatic density, it was found that temperature and type of second phase influence on the hydrostatic density values, noting lower hydrostatic density for the biomaterial with 5% SiO_2 in the HA matrix (1.38 cm^3 ± 0.02) and consequently higher value of open porosity, reaching 54.03% ± 0.7.

The results obtained by scanning electron microscopy (SEM) also revealed the presence of a significant microporosity for the HA matrix and nanocomposites biomaterials HA/SiO_2 and HA/ZrO_2 obtained in the sintering temperature 1100°C/2h, as can be seen in the micrographs represented by **Fig. 1, 2** and **3** and in **Table 1**.

Table 1. Theoretical density, hydrostatic density and open porosity measurements obtained on the sintered biomaterials.

Biomaterials	d_{th} (g/cm^3)	d_h (g/cm^3)	P A (%)
HA (1100ºC/2h)	3.16	1.81 ± 0.02	40.02 ± 0.81
HA/SiO_2 (1100ºC/2h)	3.13	1.38 ± 0.02	54.03 ± 0.77
HA/ZrO_2 (1100ºC/2h)	3.29	2.04 ± 0.08	37.04 ± 1.76
HA/Al_2O_3-□ (1300ºC/2h)	3.20	2.32 ± 0.08	22.02 ± 1.54
HA/ZrO_2 (1300ºC/2h)	3.29	3.32 ± 0.03	0.99 ±0.61

Conclusion

The development of calcium phosphate nanocomposites as biomaterials is a well-researched topic and has generated new perspectives as biomaterials for repairing and replacement of bone tissue. These new biomaterials can be used in orthopedics, traumatology and in dentistry, as a matrix element and fill defects in bone reconstruction. Interest in the development of hydroxyapatite matrix nanocomposite biomaterials is associated with the mechanical properties, with the purpose of application in regions that require high load and physical properties, such as microporosity, grain surface area and micropores, also with application interest as bone substitutes for repairing and bone reconstruction. The HA, HA/SiO_2, HA/ZrO_2 biomaterials obtained by sintering at 1100ºC/2h present similarly interconnected microporous microstructure, formed by fine grains. Calcium phosphate matrix nanocomposites are biomaterials with microporous microstructures which can be used for bone replacements and will generate innovative results as biomaterials for bone formation in surgical procedures. The physical characterization showed that the biomaterials are made of HA and TCP-β phases, however it was also observed in HA/Al_2O_3-α nanocomposite biomaterial small concentrations of tricalcium aluminate. The results of open porosity and hydrostatic density also showed that HA and HA/SiO_2, HA/ZrO_2 and HA/Al_2O_3–α nanocomposites biomaterials offer potential microporous interconnected microstructures. The HA/ZrO_2 biomaterial sintered at 1300ºC/2h, presented with less open porosity and better densification. Further studies should be done about this biomaterial; it may be developed for applications such as dental implants or surgical fixation plates. The results of this study are encouraging and show that the HA matrix nanocomposites biomaterials, with SiO_2, ZrO_2 e Al_2O_3-α as nanometric second phase in small concentrations, can offer biomaterials with fairly similar architectures to the bone structure, which could be a differential between bone tissue replacement and repairing biomaterials in surgical applications in the near future.

Acknowledgements

CNPq for the scholarship PQ and FAPESC, for the financial support to the research project in Biomaterials.

References

1. Camargo, N. H. A; Corrêa , P. ; Franczak, P. F. ; Gemelli, E. *Advances in Science and Technology*, **2014**, *87*, 61. **DOI:** 10.4028/www.scientific.net/AST.87.61
2. Santos, R. B. Síntese e Caracterização de Pós Nanoestruturados de Fosfato de Cálcio e Nanocompósitos Hidroxiapatita/Sílica-Gel Dissertação Mestrado, UDESC - Joinville, p. 89, **2009**.
3. Delima, S.A.; Camargo, N.H.A.; Souza, J.C.P.; Gemelli, E. *Synthesis and Characterization of Nanocomposites Powders Calcium Phosphate/Titanium Oxyde for Biomedical Applications*. Seventh International Latin American Conference on powder Technology, 2009, Atibaia. v. 1. p. 913-918, 2009.
4. Kumta, P.N., Sfeir, C., Lee, D., Olton, D., Choi, D. *Acta Biomaterialia*, **2005**, *1*, 65. **DOI:** 10.1016/j.actbio.2004.09.008
5. Raynaud, S.; Champion, E., Bernache-Assollant, D., Thomas, P. *Biomaterials*, **2002**, *23*, 1065. **DOI:** 10.1016/S0142-9612(01)00218-6
6. Camargo, N.H.A.; Franczak, P.F.; Gemelli, E.; Costa, B.D.; Moraes, A.N. *Advanced Materials Research*, **2014**, *936*, 687. **DOI:** 10.4028/www.scientific.net/AMR. 936.687
7. Camargo, N.H.A., Delima, S.A., Aguiar, J.F., Gemelli, E. Tomiyama, M., Synthesis and Characterization of Nanostructures Calcium Phosphates Powders and Calcium Phosphates/α-Al_2O_3 Nanocomposites. *Journal of Advanced Materials*, **2009**, 41, 33.
8. Delima, S. A.; Souza, J. C. P.; Camargo, N.H. A.; Pupio, F.; Santos, R. B. M.; Gemelli, E. Congresso Latino Americano de Órgãos Artificiais e Biomateriais, Ouro Preto, Brasil, 6, **2008**.
9. Camargo, N. H. A.; Bellini, O. J.; Gemelli, E.; Tomiyama, M. *Revista Matéria*, **2007**, *12*, 574.
10. Bellini, O. J. Síntese e Caracterização de uma Matriz Óssea de Fosfato de Cálcio e Nanocompósitos Fosfato de Cálcio/SiO_2n para Substituição e Regeneração Óssea. Dissertação de Mestrado UDESC - Joinville, p. 101, **2007**.
11. Camargo, N. H. A.; Delima, S.A.; Souza, J.C.P.; De Aguiar, J.F.; Gemelli, E.; Meier, M. M.; Silva, V.E.; Mittelstadt, F. *Key Engineering Materials*, **2009**, *396*, 619. **DOI:** 10.4028/www.scientific.net/KEM.396-398.619
12. Borba, E.E.G.; Camargo, N. H. A.; Franczak, P. F.; Gemelli, E. Síntese e caracterização de um pó cerâmico de fosfato de cálcio: Elaboração de pós nanocompósitos. 58º Congresso Brasileiro de Cerâmica 18-21 Maio, **2014**, Bento Gonçalves – RS, p. 1-12.
13. Pennings, E.C.M.; Grellner, W. *Journal American Ceramic. Society*, **1989**, *72*, 1268. **DOI:** 10.1111/j.1151-2916.1989.tb09724.x
14. Corrêa, Pricyla. Síntese e Caracterização de Nanocompósitos HA/Al_2O_3-α Sol-Gel Para Aplicações na Reconstrução óssea. Dissertação de Mestrado, UDESC - Joinville, p. 134, **2013**.
15. Camargo, N. H. A.; DeLima, S. A.; Gemelli, Enori. *American Journal of Biomedical Engineering*, **2012**, 2, 41. **DOI:** 10.5923/j.ajbe.20120202.08
16. Behnamghader, A; Bagheri, N; Raissi, B; Moztarzadeh, F. *Journal of Material Science: Material Medical*, **2008**, 19, 197. **DOI:** 10.1007/s10856-007-3120-8
17. Heimann, R. B.; Vu, T. A. *Journal of Materials Science Letters*, **1997**, 16, 437. **DOI:** 10.1023/A:1018591605388
18. Bang-Yen Chou; Edward Chang. *Biomaterials*, **1999**, 20, 1823. **DOI:** 10.1016/S0142-9612(99)00078-2